

This copy is for your personal, non-commercial use only.

If you wish to distribute this article to others, you can order high-quality copies for your colleagues, clients, or customers by [clicking here](#).

Permission to republish or repurpose articles or portions of articles can be obtained by following the guidelines [here](#).

The following resources related to this article are available online at www.sciencemag.org (this information is current as of April 21, 2010):

Updated information and services, including high-resolution figures, can be found in the online version of this article at:

<http://www.sciencemag.org/cgi/content/full/327/5967/866>

Supporting Online Material can be found at:

<http://www.sciencemag.org/cgi/content/full/327/5967/866/DC1>

A list of selected additional articles on the Science Web sites **related to this article** can be found at:

<http://www.sciencemag.org/cgi/content/full/327/5967/866#related-content>

This article **cites 16 articles**, 10 of which can be accessed for free:

<http://www.sciencemag.org/cgi/content/full/327/5967/866#otherarticles>

This article appears in the following **subject collections**:

Microbiology

<http://www.sciencemag.org/cgi/collection/microbio>

Biomedical Imaging Core Facility of the Citigroup Biomedical Imaging Center at Weill Cornell Medical College, Rafael Oania, a generous gift by the Dr. Mortimer D. Sackler family and support from NIH grants MH079513 (B.J.C., F.S.L.), MH060478 (B.J.C.), NS052819 (F.S.L.), HD055177 (B.J.C., S.S.P.), GM07739 (F.S.), and United Negro College Fund–Merck Graduate Science Research Dissertation Fellowship

(F.S.), Burroughs Wellcome Foundation (F.S.L.), and International Mental Health Research Organization (F.S.L.).

Supporting Online Material

www.sciencemag.org/cgi/content/full/science.1181886/DC1
Materials and Methods
SOM Text

Figs. S1 to S5
Tables S1 and S2
References

14 September 2009; accepted 28 December 2009
Published online 14 January 2009;
10.1126/science.1181886
Include this information when citing this paper.

Vibrio cholerae VpsT Regulates Matrix Production and Motility by Directly Sensing Cyclic di-GMP

Petya V. Krasteva,¹ Jiunn C. N. Fong,² Nicholas J. Shikuma,² Sinem Beyhan,² Marcos V. A. S. Navarro,¹ Fitnat H. Yildiz,^{2*} Holger Sondermann^{1*}

Microorganisms can switch from a planktonic, free-swimming life-style to a sessile, colonial state, called a biofilm, which confers resistance to environmental stress. Conversion between the motile and biofilm life-styles has been attributed to increased levels of the prokaryotic second messenger cyclic di-guanosine monophosphate (c-di-GMP), yet the signaling mechanisms mediating such a global switch are poorly understood. Here we show that the transcriptional regulator VpsT from *Vibrio cholerae* directly senses c-di-GMP to inversely control extracellular matrix production and motility, which identifies VpsT as a master regulator for biofilm formation. Rather than being regulated by phosphorylation, VpsT undergoes a change in oligomerization on c-di-GMP binding.

In *Vibrio cholerae*, biofilm formation is facilitated by colonial morphotype variation (1–4). Rugose variants produce increased levels of extracellular matrix by means of expression of *Vibrio* polysaccharide (*vps*) genes and genes encoding matrix proteins. *vps* expression is under the control of two positive transcriptional regulators, VpsT and VpsR (5, 6). VpsT is a member of the FixJ, LuxR, and CsgD family of prokaryotic response regulators, typically effectors in two-component signal transduction systems that use phosphoryl transfer from upstream kinases to modulate response-regulator protein activity (7–9). Although the putative phosphorylation site is conserved in VpsT's receiver domain, other residues crucial for phosphotransfer-dependent signaling are not, and no cognate kinase has been identified to date (fig. S1). Regulation by VpsT and VpsR has been linked to signal transduction by using the bacterial second messenger cyclic di-guanosine monophosphate (c-di-GMP) (10, 11) (fig. S2), yet little is known about the direct targets of the nucleotide. A riboswitch has been identified as a c-di-GMP target that regulates gene expression of a small number of genes, but that is unlikely to account for the global change in transcriptional profile required for biofilm formation (12). Neither do PilZ domain-containing proteins, potential c-di-GMP effectors, affect rugosity, because a *V. cholerae*

strain lacking all five PilZ domain-containing proteins retains its colony morphology and ability to overproduce *vps* gene products (13).

VpsT consists of an N-terminal receiver (REC) domain and a C-terminal helix-turn-helix (HTH) domain, with the latter mediating DNA binding (Fig. 1A) (14) (also see supporting online text for details). Unlike other REC domains, the canonical (α/β)₅-fold in VpsT is extended by an additional helix at its C terminus [helix α_6 in (Fig. 1A)]. The HTH domain buttresses an interface formed by helices 3 and 4 of the N-terminal regulatory domain. There are two nonoverlapping dimerization interfaces between noncrystallographic VpsT protomers [chain A-chain B and chain A-chain B^{sym} (symmetrical) in (Fig. 1B)]. The c-di-GMP-independent interface involves interactions mediated by a methionine residue (M¹⁷) (15) located at the beginning of α_1 and a binding pocket that extends into the putative phosphorylation site of the REC domain (fig. S3A). The second interface involves α_6 of the REC domain, in contrast to canonical response regulators, such as CheY and PhoB, that utilize a surface formed by α_4 - β_5 - α_5 for dimerization (9). The binding of two intercalated c-di-GMP molecules to the base of α_6 stabilizes VpsT dimers using this interface (Fig. 1 and fig. S3B).

The binding motif for c-di-GMP in VpsT consists of a four-residue-long, conserved W[F/L/M][T/S]R sequence (15) (fig. S1). The side chains of the tryptophan and arginine form π -stacking interactions with the purine rings of the nucleotide (Fig. 1C). While the hydrophobic residue in the second position plays a structural role where it is buried in the REC domain, the

threonine residue at position 3 forms a hydrogen bond with the phosphate moiety of c-di-GMP. A subclass of VpsT and/or CsgD homologs exists with a proline substitution in position 3 (W[F/L/M]PR). Although CsgD is also functionally linked to c-di-GMP signaling in *Escherichia coli* and *Salmonella* (16, 17), its binding pocket appears to be distinct from that of VpsT, as it displays a highly conserved YF[T/S]Q motif that is unlikely to accommodate c-di-GMP (fig. S3B).

The apparent affinity of VpsT for c-di-GMP, determined by isothermal titration calorimetry, is 3.2 μ M with 1:1 stoichiometry, consistent with a dimer of c-di-GMP binding to a dimer of VpsT (fig. S4A). Single point mutations in the conserved c-di-GMP-binding motif (VpsT^{R134A}, VpsT^{W131F}, or VpsT^{T133V}) or in the isoleucine in α_6 of the c-di-GMP-stabilized REC dimerization interface (VpsT^{T141E}) abolished c-di-GMP binding, which indicated that dimeric REC domains are required for binding (fig. S4B). Conversely, mutation of a key residue in the nucleotide-independent interface (VpsT^{M17D}) had no effect on c-di-GMP recognition. On the basis of static multiangle light scattering, VpsT^{M17D} exists as a monomeric species in the absence of c-di-GMP, whereas intermediate molecular weights for the wild-type VpsT and the mutants VpsT^{R134A} and VpsT^{T141E} indicated fast exchange between monomers and dimers, presumably through the c-di-GMP-independent interface (fig. S5 and table S2). Addition of c-di-GMP increases the molecular weight of VpsT^{M17D} and wild-type VpsT (figs. S5 and S6), whereas the oligomeric state of VpsT^{R134A} and VpsT^{T141E} is insensitive to the nucleotide.

The role of c-di-GMP recognition and the relevance of the two dimer interfaces in DNA-binding and VpsT-regulated gene expression were assessed by using c-di-GMP binding (R¹³⁴) and dimerization (I¹⁴¹ or M¹⁷) mutants (Fig. 2). In electromobility shift assays, we used regulatory sequences upstream of *vpsL*, a gene under positive control of VpsT (Fig. 2A) (6). DNA mobility shifts were observed only for the wild-type and VpsT^{M17D} forms, where the effect was protein specific and c-di-GMP dependent. In addition, nucleotide-dependent DNA binding of VpsT was observed to multiple and relatively remote sites in the regulatory region of *vpsL*.

To evaluate the functional importance of VpsT oligomers and c-di-GMP binding in cells, we measured transcription of *vps* genes by using a chromosomal *vpsLp-lacZ* transcriptional fusion in the Δ *vpsT* strain harboring wild-type *vpsT*, *vpsT* point mutants (VpsT^{M17D}, VpsT^{R134A}, or

¹Department of Molecular Medicine, College of Veterinary Medicine, Cornell University, Ithaca, NY 14853, USA. ²Department of Microbiology and Environmental Toxicology, University of California, Santa Cruz, CA 95064, USA.

*To whom correspondence should be addressed: yildiz@metx.ucsc.edu (F.H.Y.); hs293@cornell.edu (H.S.)

vpsT^{I141E}) or the insertless expression vector (pBAD) (Fig. 2B). The presence of wild-type VpsT and VpsT^{M17D} resulted in increased *vpsL* expression, similar to that from the wild-type rugose strain carrying vector only, whereas $\Delta vpsT$ strains with VpsT^{R134A}, VpsT^{I141E}, or the empty vector did not exhibit such an increase. These data confirm that c-di-GMP-mediated oligomerization is critical for VpsT function. Mutations in the putative phosphorylation site designed to produce a constitutively inactive or active state, VpsT^{D60A} or VpsT^{D60E}, respectively, did not alter the efficiency of VpsT significantly. Hence, regulation of gene expression is presumably independent of phosphorylation of VpsT (see fig. S7).

Next, we determined the gene regulatory potential as a function of c-di-GMP binding and oligomerization through whole-genome expression profiling by comparing a $\Delta vpsT$ strain expressing either wild-type VpsT or VpsT point mutants (VpsT^{M17D}, VpsT^{R134A}, or VpsT^{I141E}) with that of cells harboring the pBAD vector alone (Fig. 2C and table S3). Genes located in the *vps*-I and *vps*-II clusters, as well as the *vps* intergenic region, were strongly induced when wild-type VpsT and VpsT^{M17D} were expressed, and significantly less so in the strains expressing VpsT^{R134A} or VpsT^{I141E}. We also observed that the expression of several genes encoding flagellar proteins was decreased in cells express-

ing wild-type VpsT and VpsT^{M17D} but not in cells expressing VpsT^{R134A} or VpsT^{I141E}, which suggested that VpsT inversely regulates motility and matrix production in a c-di-GMP-dependent manner (Fig. 2C and fig. S7). These results were corroborated in motility assays, in which a $\Delta vpsT$ strain or strains expressing c-di-GMP-binding mutants showed increased migration on soft agar plates compared with rugose strains that express VpsT forms that are capable of c-di-GMP-dependent dimerization (Fig. 3A).

The strain harboring VpsT^{M17D} had an expression profile similar to that of the strains harboring wild-type VpsT, however, with increased magnitude, which indicated that c-di-GMP-independent dimerization could be inhibitory or regulatory (Fig. 2, A and C). In contrast, the c-di-GMP-dependent interaction between two VpsT monomers is sufficient and necessary for DNA recognition and transcriptional regulation.

The corrugated appearance of rugose colonies can be attributed largely to increased levels of exopolysaccharides, which are induced by VpsT (6). As a consequence, *V. cholerae* mutants lacking *vpsT* produce smooth and flat colonies (Fig. 3B). To elucidate phenotypic consequences of mutations that abolish c-di-GMP binding and/or dimerization of VpsT, we compared the colony morphology of a $\Delta vpsT$ strain harboring wild-type VpsT with that of one of the point

mutants described above. Expression of wild-type VpsT and VpsT^{M17D} resulted in smooth-to-rugose conversion, where spot corrugation was greater in a $\Delta vpsT$ strain harboring VpsT^{M17D} compared with a strain with wild-type VpsT. Introduction of VpsT^{R134A}, VpsT^{I141E}, or a double-mutant VpsT^{M17D/R134A} failed to promote the smooth-to-rugose switch, but led to a distinct phenotype, characterized by increased spot diameter and weak corrugation, with a notable radial pattern (Fig. 3B and fig. S8).

Cyclic di-GMP in the rugose variant is required for increased *vps* and *vpsT* gene expression (10, 11), which suggests that VpsT is involved in a positive-feedback loop that integrates c-di-GMP to produce a robust transcriptional response. Robust matrix and biofilm formation rely on the mutual dependence of VpsT and VpsR, with VpsT introducing c-di-GMP-sensitivity to the regulatory network. In contrast, the transcriptional regulator FleQ from *Pseudomonas aeruginosa*, a distant VpsR homolog, appears to sense c-di-GMP directly, and independently of a VpsT homolog by using a distinct c-di-GMP-binding motif (18).

Taken together, we establish VpsT as a transcriptional regulator that inversely regulates biofilm formation and motility by directly integrating c-di-GMP signaling. Cyclic di-GMP-driven dimerization is mediated by an extension of the canonical receiver domains, a structural motif

Fig. 1. Crystal structure of VpsT. (A) Structure of a VpsT protomer. (B) Structure of a crystallographic trimer representing two potentially relevant, nonoverlapping dimerization interfaces. Cyclic di-GMP molecules are shown as sticks; key residues mediating ligand binding and interprotomer interactions are shown as spheres. (C) Close-up view of the nucleotide binding pocket with residues involved in coordinating the ligand shown as sticks. (Left) A ($|F_{\text{obs}}| - |F_{\text{calc}}|$) electron density map contoured at 3.6σ is shown as calculated from a model before inclusion of c-di-GMP.

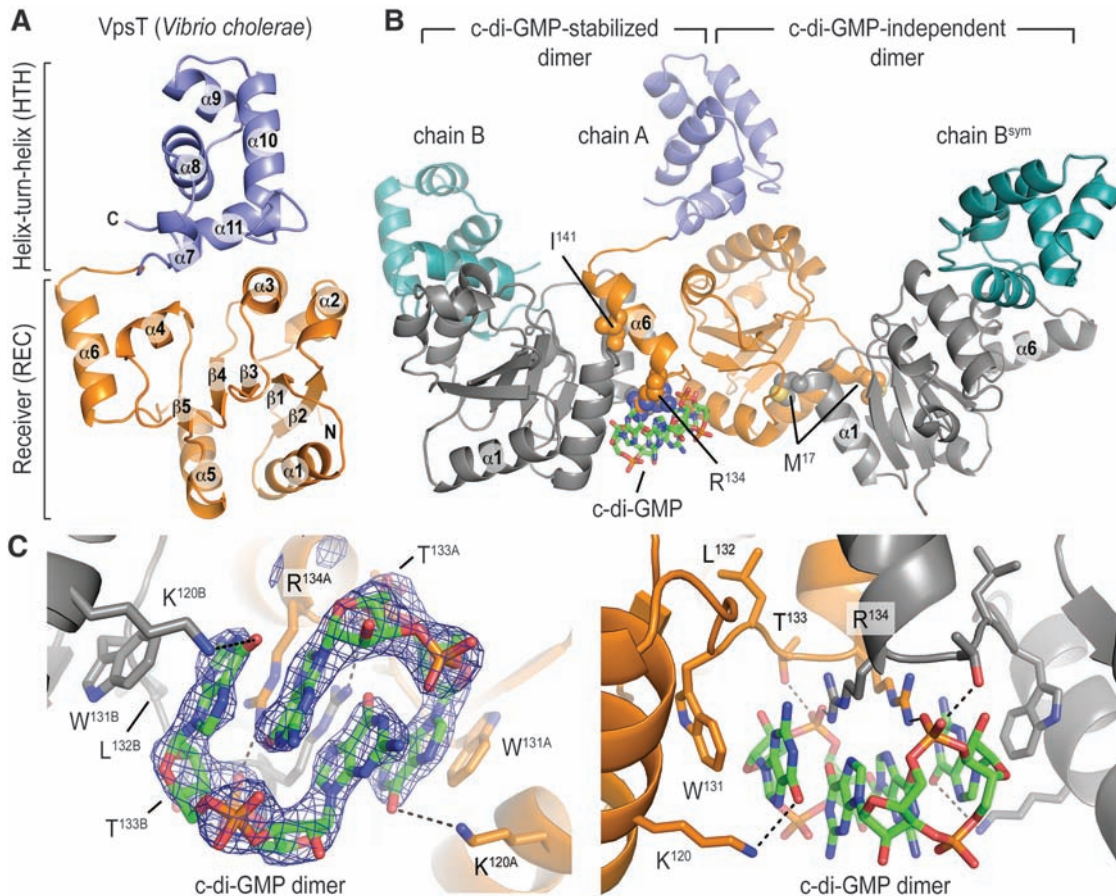


Fig. 2. Transcriptional regulation by VpsT. **(A)** Electromobility shift assays with purified proteins and biotin-labeled DNA fragments tiling the *vpsL* promoter region. Numbers indicate position relative to the open reading frame start. **(B)** *vpsL* gene expression in different genetic backgrounds harboring a single-copy chromosomal *vpsLp-lacZ* fusion. Data are means \pm SD of eight replicates. **(C)** Whole-genome expression profiling. (Top) Compact heat map in a log₂-based pseudocolor scale (yellow, induced; blue, repressed) that compares a total of 108 differentially expressed genes in a $\Delta vpsT$ strain expressing wild-type (wt) or mutated VpsT versions with the vector control. (Middle) Expression profiles of genes located in and between the *vps-I* and *vps-II* clusters; (bottom) expression profiles of flagellar biosynthesis genes.

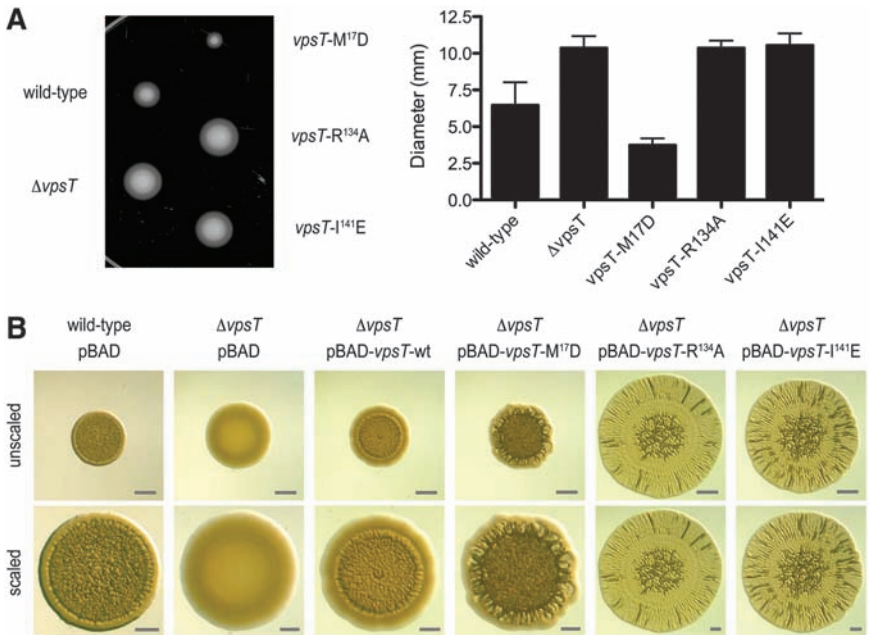
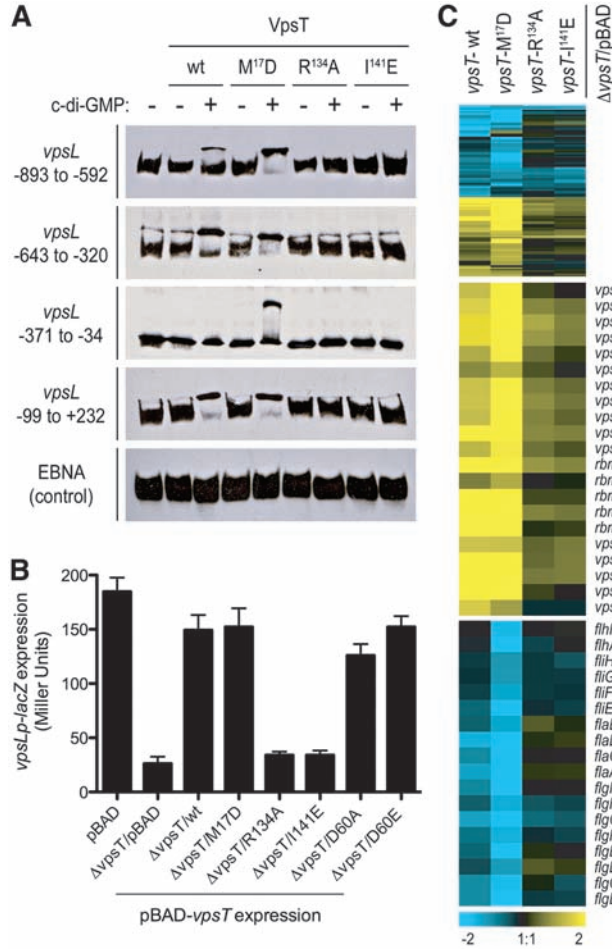


Fig. 3. Functional characterization of wild-type rugose, $\Delta vpsT$ strains, and $\Delta vpsT$ strains expressing wild-type or mutant forms of VpsT. **(A)** Motility phenotypes on semisolid Luria-Bertani broth agar plates. For strains expressing mutants of VpsT, single chromosomal insertion mutants are shown. The graph shows the mean migration zone diameter of each strain. Data are means \pm SD of 11 replicates. **(B)** Spot morphologies. A wild-type rugose strain carrying the vector (pBAD) and $\Delta vpsT$ strains carrying the vector or plasmids containing wild-type or mutant *vpsT* are shown [(top) unscaled; scale bars, 2 mm; (bottom) scaled to similar diameter; scale bars, 1 mm].

that defines a widespread class of response regulators, including CsgD and other LuxR family proteins. Although some mechanisms may only pertain to close homologs of VpsT, such as c-di-GMP-dependent dimerization, the general mode of action involving dimerization accompanied by changes in the relative orientation of the DNA binding domains is likely to be relevant for the large family of homologous transcription factors.

References and Notes

1. Y. Mizunoe, S. N. Wai, A. Takade, S. I. Yoshida, *Infect. Immun.* **67**, 958 (1999).
2. F. H. Yildiz, G. K. Schoolnik, *Proc. Natl. Acad. Sci. U.S.A.* **96**, 4028 (1999).
3. J. C. Fong, K. Karplus, G. K. Schoolnik, F. H. Yildiz, *J. Bacteriol.* **188**, 1049 (2006).
4. J. C. Fong, F. H. Yildiz, *J. Bacteriol.* **189**, 2319 (2007).
5. S. Beyhan, K. Bilecen, S. R. Salama, C. Casper-Lindley, F. H. Yildiz, *J. Bacteriol.* **189**, 388 (2007).
6. C. Casper-Lindley, F. H. Yildiz, *J. Bacteriol.* **186**, 1574 (2004).
7. N. T. Chirwa, M. B. Herrington, *Microbiology* **149**, 525 (2003).
8. U. Römling, Z. Bian, M. Hammar, W. D. Sierralta, S. Normark, *J. Bacteriol.* **180**, 722 (1998).
9. R. Gao, A. M. Stock, *Annu. Rev. Microbiol.* **63**, 133 (2009).
10. B. Lim, S. Beyhan, J. Meir, F. H. Yildiz, *Mol. Microbiol.* **60**, 331 (2006).
11. S. Beyhan, F. H. Yildiz, *Mol. Microbiol.* **63**, 995 (2007).
12. N. Sudarsan *et al.*, *Science* **321**, 411 (2008).
13. S. Beyhan, L. S. Odell, F. H. Yildiz, *J. Bacteriol.* **190**, 7392 (2008).
14. Materials and methods are available as supporting material on Science Online.
15. Single-letter abbreviations for the amino acid residues are as follows: A, Ala; C, Cys; D, Asp; E, Glu; F, Phe; G, Gly; H, His; I, Ile; K, Lys; L, Leu; M, Met; N, Asn; P, Pro; Q, Gln; R, Arg; S, Ser; T, Thr; V, Val; W, Trp; and Y, Tyr. The single point mutation R134A is a substitution of Ala for Arg¹³⁴.
16. A. Kader, R. Simm, U. Gerstel, M. Morr, U. Römling, *Mol. Microbiol.* **60**, 602 (2006).
17. H. Weber, C. Pesavento, A. Possling, G. Tischendorf, R. Hengge, *Mol. Microbiol.* **62**, 1014 (2006).
18. J. W. Hickman, C. S. Harwood, *Mol. Microbiol.* **69**, 376 (2008).
19. We are grateful to S. Hubbard and W. Horne for providing access to light scattering and calorimetry, respectively, and to the staff at the National Synchrotron Light Source (NSLS; Brookhaven National Laboratories) for assistance with synchrotron data collection. The NSLS is supported by the Offices of Biological and Environmental Research and of Basic Energy Sciences of the U.S. Department of Energy, and by the National Center for Research Resources of the NIH. This work was supported by the NIH (1R01GM081373 to H.S. and R01AI055987 to F.H.Y.), and by a PEW Scholar award (H.S.). Atomic coordinates and structure factors have been deposited in the RCSB Protein Data Bank under ID code 3KLN and 3KLO. The microarray data have been deposited in NCBI's Gene Expression Omnibus and are accessible through GEO series accession number GSE19479.

Supporting Online Material

www.sciencemag.org/cgi/content/full/327/5967/866/DC1
 Materials and Methods
 SOM Text
 Figs. S1 to S13
 Tables S1 to S4
 References

27 August 2009; accepted 17 December 2009
 10.1126/science.1181185